



REVISTA DE INGENIERIA DE LA FACULTAD DE INGENIERIA, UNIVERSIDAD NACIONAL DE COLOMBIA - BOGOTÁ

DYNA

ISSN: 0012-7353

ISSN: 2346-2183

Universidad Nacional de Colombia

Maestre-Cambronel, Daniel; Hernández-Comas, Brando; Duarte-Forero, Jorge  
Experimental and economic assessment of alkaline electrolyzer  
for dual-fuel operation in low-displacement diesel engines  
DYNA, vol. 88, no. 219, 2021, October-December, pp. 68-77  
Universidad Nacional de Colombia

DOI: <https://doi.org/10.15446/dyna.v88n219.92439>

Available in: <https://www.redalyc.org/articulo.oa?id=49671317008>

- How to cite
- Complete issue
- More information about this article
- Journal's webpage in [redalyc.org](https://www.redalyc.org)

UNEN [redalyc.org](https://www.redalyc.org)

Scientific Information System Redalyc

Network of Scientific Journals from Latin America and the Caribbean, Spain and Portugal

Project academic non-profit, developed under the open access initiative

# Experimental and economic assessment of alkaline electrolyzer for dual-fuel operation in low-displacement diesel engines

Daniel Maestre-Cambronel, Brando Hernández-Comas & Jorge Duarte-Forero

KAI Research Unit, Programa de Ingeniería Mecánica, Universidad del Atlántico, Barranquilla, Colombia. dmaestre@est.uniatlantico.edu.co, bhernandezc@mail.uniatlantico.edu.co, jorgeduarte@mail.uniatlantico.edu.co

Received: December 18<sup>th</sup>, 2020. Received in revised form: July 23<sup>th</sup>, 2021. Accepted: September 7<sup>th</sup>, 2021.

## Abstract

This investigation evaluated the integration of an alkaline electrolyzer for dual-fuel operation in an experimental test bench of a diesel engine from a techno-economic viewpoint. The characterization of the electrolyzer operation indicated that higher electrolyte (KOH) concentrations (30 – 40% w/w) improve the overall performance since less voltage is required for electrolysis, thus featuring higher efficiencies (50 – 60%) and hydrogen production (4 – 6 LPM). The economic analysis demonstrated that hydrogen cost remains competitive (4.3 - 5.6 USD/kg), and it is greatly dependent on the electrolyte concentration. Additionally, the operation of the engine with hydrogen injection at 20 LPM and a palm biodiesel blend reduced the fuel consumption rate between 10 – 31% depending on the load rate when compared to pure diesel. In contrast, dual-fuel operation generated a minor reduction in fuel conversion efficiency (< 5%), which reflects on the power output. Overall, this technology stands as a promising avenue to improve the fuel utilization ratio.

**Keywords:** alkaline electrolyzer; diesel engine; economic analysis; fuel consumption; hydrogen.

## Evaluación experimental y económica de un electrolizador alcalino para operación dual en motores diésel de baja cilindrada

### Resumen

Esta investigación evaluó la integración de un electrolizador alcalino para la operación con combustible dual en un banco de pruebas experimental de un motor diésel desde un punto de vista tecno-económico. La caracterización de la operación del electrolizador indicó que concentraciones más altas de electrolitos (KOH) (30 – 40% p/p) mejoran el rendimiento general, ya que se requiere menos voltaje para la electrólisis, lo que presenta mayores eficiencias (50 – 60%) y producción de hidrógeno (4 – 6 LPM). El análisis económico demostró que el costo del hidrógeno sigue siendo competitivo (4.3 – 5.6 USD/kg) y depende en gran medida de la concentración de electrolitos. Además, el funcionamiento del motor con inyección de hidrógeno a 20 LPM y una mezcla de biodiesel de palma redujo la tasa de consumo de combustible entre un 10 – 31% dependiendo de la tasa de carga, en comparación con el diésel puro. Por el contrario, el funcionamiento con combustible dual generó una reducción menor en la eficiencia de conversión de combustible (< 5%), lo que se refleja en la potencia de salida. En general, esta tecnología se presenta como una vía prometedora para mejorar el índice de utilización de combustible.


**Palabras claves:** análisis económico; consumo de combustible; electrolizador alcalino; hidrógeno; motor diésel.

### 1. Introduction

The imminent growth of the world population has generated a dramatic increase in global energy demand, which represents a substantial problem since most of the energetic systems are driven by non-renewable energy sources. Internal Combustion Engines (ICE) stand as one of

the most relevant thermal machines due to their versatile applications in industry, agriculture, transportation, and power generation [1-3]. Consequently, ICEs contribute to a substantial share of the global CO<sub>2</sub> emissions, which has promoted severe governmental policies and challenging efforts to reduce the greenhouse emissions inherent in operation [4,5].

**How to cite:** Maestre-Cambronel, D., Hernández-Comas, B. and Duarte-Forero, J., Experimental and economic assessment of alkaline electrolyzer for dual-fuel operation in low-displacement diesel engines.. DYNA, 88(219), pp. 68-77, October - December, 2021.

© The author; licensee Universidad Nacional de Colombia.   
Revista DYNA, 88(219), pp. 68-77, October - December, 2021, ISSN 0012-7353  
DOI: <https://doi.org/10.15446/dyna.v88n219.92439>

Renewable energy systems have emerged as a promising avenue to decelerate global warming while providing diversification of the global energy market [6,7]. Despite the advantages and progress towards clean energy systems, these technologies only account for 5-10% of the worldwide energy production [8]. In contrast, energy systems powered by fossil fuels overcome more than 50%, which demonstrates the immediate necessity to promote reliable solutions to mitigate the adverse effects of these practices [9]. Specifically, the overall efficiency of ICEs in terms of thermo-mechanical performance can be improved by the incorporation of alternative fuels. Hence, various biofuels blends have been proposed from different raw materials such as vegetable oils and animal fats. This technique is increasing interest due to the simplicity and suitable incorporation in ICEs without major modifications [10,11]. Also, the physicochemical characteristics of biodiesel blends are most likely compatible with those of conventional diesel, which reinforces its implementation [12].

Sathiyamoorthi et al. [9] introduced a Palmarosa biodiesel blend in a diesel engine, encountering a significant reduction in the overall emissions of smoke, CO, and HC opacity. In contrast, the study revealed that NOx emissions increase by around 20-40%, depending on the operating margin. Uyumaz et al. [13] examined the influence of tire oil biodiesel blends when implemented in a direct injection diesel engine. The authors stated that biodiesel incorporation reduces the overall emissions between 50-70% but intensifies the fuel consumption by approximately 15.8% compared to pure diesel.

The study on emissions control is quite extensive, and most of the studies agreed that biodiesel blends reduce a great share of greenhouse emissions [10]. NOx emissions appeared to be the negative effect of this technique; therefore, upcoming studies center on the exploration of new blends that guarantee maximum global emissions minimization. Despite the intensive investigation towards fuel consumption metrics as a tool to reveal the influence of biodiesel incorporation, some conflicts can be found on the criteria. In contrast, a limited explanation of this phenomenon is incorporated since the main focus relies on emissions control. The latter demonstrates that there is a significant necessity to generate a comprehensive understanding of this matter.

On the other hand, hydrogen plays an important role as a prospective cleaner fuel that facilitates energy transition [14,15]. Indeed, hydrogen technologies are becoming of increasing interest for both academics and industries due to their reliable operation as an energy carrier [16,17]. Particularly, the role of hydrogen in ICEs is intended to minimize the issues related to greenhouse emissions while maintaining thermal requirements related to the combustion phenomena [18].

Natural gas decomposition is one of the most profitable and massive technologies, with nearly 60% of the global production [19]. However, this technology possesses a significant carbon footprint related to the collateral emissions of greenhouse gases inherent to its production [8]. Therefore, the new conceptualization of production practices is driven to obtain the so-called green-hydrogen. Water electrolysis has become the most common technology to produce hydrogen, with nearly 99.99% pureness at zero emissions [20]. Alkaline electrolyzers stand as a mature technology that offers simplified operation with

reasonable efficiencies and investment costs [14].

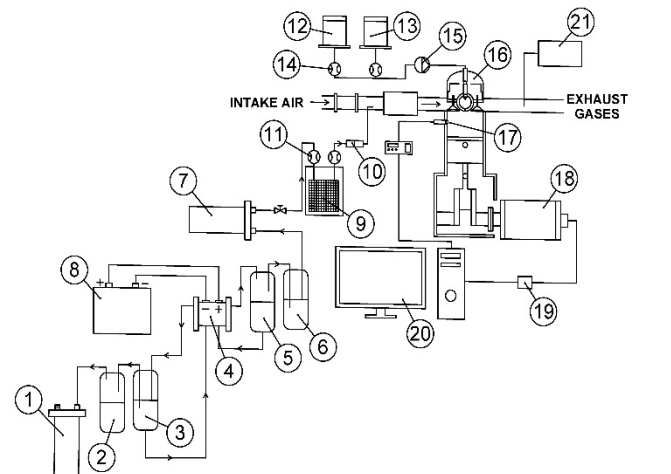
Recently, Thiyagarajan et al. [21] incorporated an electrolyzer into a hybrid system comprising a diesel engine and a thermoelectric generator. Experimental tests were carried out that showed significant improvements in fuel consumption and emissions. Most studies that include partial fuel substitution with hydrogen rarely characterize the production mechanism. At the same time, the economic perspectives remain unexplored even though it stands as a suitable tool to foster its commercialization and implementation [22]. Therefore, the differential factor of this investigation can be found in the integration of an in-house alkaline electrolyzer for dual-fuel operation in diesel engines while considering techno-economic criteria.

The present investigation presents an experimental assessment of dual-fuel operation in diesel engines, namely hydrogen injection and Palm biodiesel blend (B10). Additionally, the study incorporates a complete characterization of the hydrogen production process from a techno-economic perspective, representing a unique aspect from former research. Therefore, this work contributes to close the knowledge gap associated with fueling consumption metrics in partial fuel substitution techniques while integrating hydrogen technologies in the experimental test bench. Accordingly, the next section describes the main features of the experimental test bench. Later, Section 3 provides a detailed explanation of the techno-economic modeling implemented in the study. Section 4 highlights the main results and discussions. Finally, Section 5 provides the concluding statements and future work suggestions.

## 2. Experimental Setup

### 2.1 System description

Fig. 1 shows the schematic representation of the experimental test bench. The main components of each of the subsystems are outlined.



1. Oxygen storage tank 2. Oxygen electrolytic tank, 3. Oxygen bubbler, 4. Monopolar alkaline cell, 5. Hydrogen electrolytic tank, 6. Hydrogen bubbler, 7. Hydrogen storage tank, 8. AC/DC converter, 9. Flame arrester, 10. Silica gel filter, 11. Hydrogen flowmeter, 12. Diesel tank, 13. Biodiesel tank, 14. Fuel flowmeter, 15. Fuel pump, 16. Diesel engine, 17. Pressure sensor, 18. Alternator, 19. Encoder, 20. Data acquisition system, 21. Exhaust gases analyzer.

Figure 1. Schematic of the experimental test bench.

Source: The authors.



Figure 2. Experimental test-bench of the study.  
Source: The authors.

Table 1.  
Instruments used for measurements

Engine	Variable	Range	Accuracy
<b>Instrument</b>			
Power analyzer PCE-PA6000	Power	1W – 999.99 kW	±1.5 %
Gravimetric meter	Fuel mass Flow rate	0 – 16 g/s	±2%
Mass flow meter hot wire	Air mass Flow rate	0–125 g/s	±1.2%
Temperature Thermocouple Type K	Temperature	-40 to 1100°C	±0.7%
Digital Barometer	Atmospheric Pressure	30 kPa to 110 kPa	±2%
<b>Electrolyzer</b>			
Pressure Transmitter Model A-10	Pressure	0 to 1,000 bar	±0.5%
Temperature Thermocouple Type K	Temperature	-40 to 1100°C	±0.1%
Flow Meter GT-556-MTR-ICV	Hydrogen Flow	Up to 8 L/min	±1.2%

Source: The authors.

Fig. 2 shows a picture of the experimental bank of the study, and Table 1 lists the attributes of the measuring instruments utilized in the experimental test bench. The next section presents a complete characterization of each subsystem to define the main features of the operation.

## 2.2 Diesel Engine

The experimental assessment was conducted on a single-cylinder, direct-injected, air-cooled, naturally aspirated, four-stroke diesel engine. The details of the technical characteristics of the engine are listed in Table 2.

A load bank has been incorporated in the experimental setup to emulate the operational load that the engine experience in actual applications. This allows controlling engine speed, uses power blocks of 335 W and 660 W, and has an upper power limit of 3.5 kW.

Table 2.  
Technical specifications of the engine.

Model	SK-MDF300
Manufacturer	SOKAN
Cylinder diameter	78 mm
Stroke	63 mm
Cycle	4 - stroke
Volume displacement	300 cc
Top power	3.43 kW
Injection mechanism	Direct injection
Intake mechanism	Naturally aspirated

Source: The authors.

## 2.3 Alkaline Electrolyzer

The hydrogen production within the experimental test bench is powered by a monopolar alkaline electrolyzer displayed in Fig. 3. The main features of the in-house designed electrolyzer are listed in Table 3. Notice that only the hydrogen flow is implemented in the analysis. Therefore, the oxygen is stored in a tank.

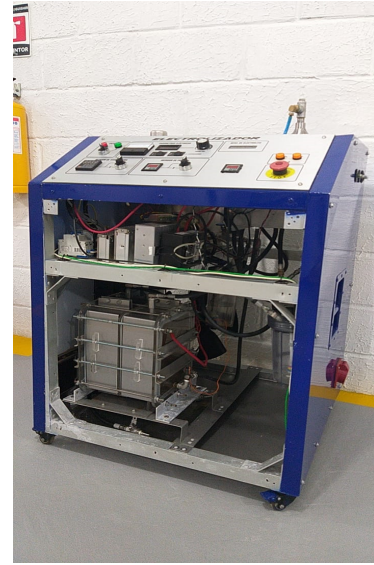


Figure 3. Hydrogen generation bench.  
Source: The authors.

Table 3.  
Technical specifications of the engine.

Specification	Value/type
Electrolyte	KOH solution
Electrolyte capacity	10 L
Solution temperature	40–50 ° C
Body Material	PMMA
Electrode material	Stainless steel 304,
	0.8 mm
Electrode orientation	Vertical
Active electrode area	32 cm <sup>2</sup>
Electrode spacing	3 mm
Number of electrodes in the cathodic chamber	18
Number of electrodes in the anodic chamber	18

Source: The authors.

The hydrogen generation system has an electrolytic tank, which continuously supplies a flow of water directed to the dry cell. In this way, the continuous generation of hydrogen is guaranteed. A bubbler tank was used to trap the water vapor mixed with the hydrogen, which protects the engine from corrosion. The hydrogen produced is stored in tanks designed and manufactured following Section VIII Division 1 of the ASME Code for Pressure Vessels. For the safety of the hydrogen generation system, a silica gel filter was installed to retain the gas's moisture. Additionally, two arresters were used to prevent the backflow of the flame. A gas analyzer is used to evaluate the composition of the gas produced. The results show a 99% hydrogen purity. The hydrogen generation system was made of stainless steel 304 due to its high corrosion resistance.

## 2.4 Fuels

The study incorporates a dual-fuel operation mode for the diesel engine. Accordingly, a biodiesel blend of palm oil was mixed with pure diesel in a 10:1 proportion (B10). In addition, hydrogen enrichment is incorporated by intake air injection in volumetric a volumetric flow of 20 LPM. The selection of the volumetric flow is validated with the autodetonation tendency, as outlined in Section 3.2. The main properties of each of the tested fuels are listed in Table 4.

Table 4.  
Properties of the tested fuels.

Properties	B10	Hydrogen
Calorific value (MJ/kg)	42.5	120
Density at NTP gas (kg/m <sup>3</sup> )	0.86	0.0838
Lower flammability limit (Vol% in air)	0.7	4
Upper flammability limit (Vol% in air)	5	75
Research octane number	-	>130
Auto-ignition temperature (°C)	553	858
Stoichiometric A/F (kg of air/kg of fuel)	14.5	34
Flame speed (m/s)	0.3	2.7
Cetane number	45	-
Specific gravity	0.83	0.091
Boiling point (K)	560	20.27

Source: The authors.

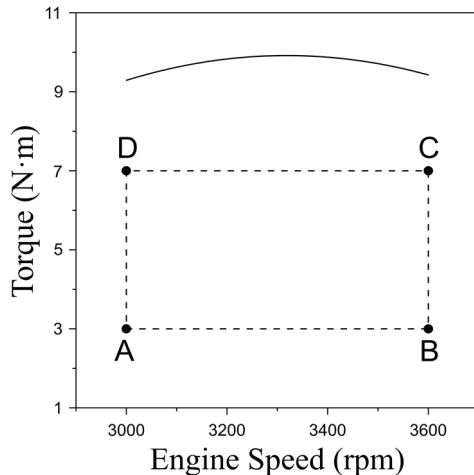


Figure 4. Operation modes selected for the experimental assessment.  
Source: The authors.

## 2.5 Operation Procedure

For the experimental tests, four modes of operation were established, as shown in Fig. 4. Each mode was strategically chosen to cover a large range of the engine operation area that further characterize the emissions levels and fuel consumption rate.

The operation modes of the analysis have been identified with the letters A, B, C, and D. Analyzing the influence of partial fuel substitution on the greenhouse emissions represents a key factor for unrevealing the positive effects of this technology.

## 3. Techno-economic modeling

### 3.1 Combustion and fuel consumption metrics

The combustion phenomena of compression ignition engines are pretty complex due to the inherent influence of different variables such as fuel properties, combustion chamber design, injection system, operating conditions, among others. The stoichiometric relation of air/fuel can be defined as follows [23]:

$$(A/F)_{esteq} = \left( \frac{m_{air}}{m_{fuel}} \right) = \frac{4.76 \cdot a \cdot PM_{air}}{1 \cdot a \cdot PM_{fuel}} \quad (1)$$

where  $PM_{air}$  and  $PM_{fuel}$  are the molecular weight of air and fuel, respectively. Similarly,  $m_{air}$  and  $m_{fuel}$  The term "a" represents the stoichiometric molar value of oxygen. Relates the mass of air and fuel, respectively. The equivalence ratio ( $\Phi$ ) (eq. (2)) is used to quantitatively parametrized if the air/fuel mixture is poor ( $\Phi < 1$ ), rich ( $\Phi > 1$ ) or ideal ( $\Phi = 1$ ) [23]:

$$\Phi = \frac{(A/F)_{esteq}}{(A/F)} \quad (2)$$

The brake-specific dual-diesel fuel consumption (BSDFC) relates the engine operation with respect to the dual-fuel operation. Accordingly, when the engine operates with pure diesel, this parameter can be expressed as the unity as can be seen in eq. (3) [23]:

$$BSDFC(g/kWh) = \frac{\dot{m}_{diesel,dual}}{P_{br}} \quad (3)$$

where  $\dot{m}_{diesel,dual}$  represents the mass flow of the dual-fuel and  $P_{br}$  refers to the brake power. Notice that the brake specific fuel consumption (BSFC) indicates fuel consumption when the engine operates with pure diesel, and it is calculated employing eq. (3).

On the other hand, the brake-specific fuel consumption efficiency (BFCE) relates the brake power to the energy released during combustion. It can be calculated as follows:

$$BFCE = \frac{P_{br}}{\dot{m}_{diesel,dual} \cdot LHV_{diesel} + \dot{m}_{H_2} \cdot LHV_{H_2}} \quad (4)$$

where  $LHV$  represents the low heating value of each fluid and  $\dot{m}_{H_2}$  relates the mass flow of hydrogen. Lastly, it is

necessary to characterize the effect of the amount of hydrogen that is being replaced. Hence, the hydrogen energy sharing ( $\Omega$ ) is a non-dimensional parameter that relates the ratio between the energy provided by hydrogen enrichment and the required energy for a stand-alone diesel operation mode [23]:

$$\Omega = \frac{\dot{m}_{H_2} \cdot LHV_{H_2}}{\dot{m}_{100\% \text{ diesel}} \cdot LHV_{\text{diesel}}} \cdot 100 \quad (5)$$

### 3.2 Partial fuel substitution criteria

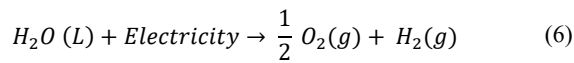
The autodetonation tendency defines the rate of partial fuel substitution with hydrogen in the engine. Amador et al. [24] proposed a predictive model to estimate the autodetonation in diesel engines based on operational and geometrical parameters. Since hydrogen is injected directly into the intake air system, this methodology aims to verify that the engine will not reach the autodetonation temperature (560°C) for the dual-fuel operation for a given condition. Table 5 displays the results of the predicted temperature at the injection point.

Based on the results, it can be verified that the autodetonation temperature remains below the limit condition for all the operation modes with hydrogen enrichment of 20 LPM.

### 3.3 Electrolyzer

This section aims to describe the main features of the electrolyzer's performance. First, it is necessary to set up basic assumptions within the analysis: (a) hydrogen and oxygen are modeled as ideal gases, (b) water fluid is assumed to be incompressible, and (c) both the liquid and gas phases remain separate.

The decomposition of water molecules can be obtained by supplying an electric current (DC) to two electrodes separated by an electrolyte (KOH) that enhances ion conductivity. The overall reaction can be expressed as follows:



Notice that oxygen production accounts to be half of that of hydrogen. In the experimental test bench, the volumetric flow of hydrogen ( $\dot{V}_{H_2}$ ) is measured with a flow meter, thus the mass flow rate ( $\dot{m}_{H_2}$ ) can be obtained via eq. (7).

$$\dot{m}_{H_2} = \dot{V}_{H_2} \cdot \rho_{H_2} \quad (7)$$

where  $\rho_{H_2}$  refers to the hydrogen density. Finally, the electrolyzer efficiency is introduced by eq. (8) to evaluate the overall performance [25].

$$\eta_{el} = \frac{\dot{m}_{H_2} \cdot LHV_{H_2}}{V \cdot I} \quad (8)$$

where  $V$  and  $I$  represent the voltage and the current of the electrolyzer, respectively.

### 3.4 Economic modeling

This section provides a framework for describing some economic metrics of the alkaline electrolyzers. The overall performance of an electrolyzer can be affected by the operating temperature, electrolyte concentration, operating voltage, and current, among others.

First, it is important to provide a cost breakdown for the construction of the equipment. Kuckshinrichs et al. [14] introduced an economic analysis to characterize the cost allocation (Fig. 5) in alkaline electrolyzers for hydrogen production plants.

Since the electrolyzer stack overcomes the most significant cost-share, Table 6 displays the cost distribution for this element.

The economic assessment presented in this study is driven to estimate the hydrogen cost based on operational conditions. This approach is commonly implemented to estimate the financial attractiveness of hydrogen technologies in the transportation sector [15]. Accordingly, the study incorporates a cost scaling approach to relate the investment cost from different manufacturers [26]. Hence, this methodology allows correlating cost estimations from different system capacities via eq. (9) [22]:

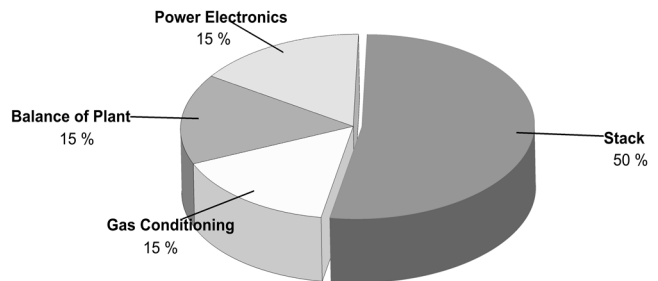


Figure 5. Alkaline electrolyzer cost breakdown.  
Source: Adapted from Kuckshinrichs et al. [14].

Table 5.  
Results of the autodetonation for different operation modes.

Test	Operation Mode	H <sub>2</sub> flow [LPM]	Autoignition Temperature [°C]
1	D	20	551
2	C	20	576
3	C	0	N/A
4	B	20	543
5	A	0	N/A
6	B	0	N/A
7	C	0	N/A
8	A	20	520

Source: The authors.

Table 6.  
Results of the autodetonation for different operation modes.

Cost breakdown in the cell stack			
Component	Value (%)	Component	Value (%)
Sealing	4	Bipolar plate	7
Pre electrode	12	Membrane	7
Anode	25	Cathode	24
Structural ring	14	Flanges	4
Tie rods	3		

Source : Adapted from Kuckshinrichs et al. [14].

$$Inv_{act} = Inv_{ref} \cdot \left( \frac{CP_{act}}{CP_{ref}} \right)^\alpha \quad (9)$$

where  $Inv_{act}$  and  $Inv_{ref}$  represents the investment cost of the actual and reference systems, respectively. In the same way,  $CP_{act}$  and  $CP_{ref}$  refers to the system capacity of the actual and reference systems, respectively. Consequently thus, the hydrogen cost ( $\dot{C}_{H_2}$ ) can be estimated by means of eq. (10) [15]:

$$\dot{C}_{H_2} = \frac{\dot{Z}_{cc} + \dot{Z}_{O\&M} + \dot{Z}_e}{E_{p,year}} \quad (10)$$

where  $\dot{Z}_{cc}$ ,  $\dot{Z}_{O\&M}$  and  $\dot{Z}_e$  represents the annualized: capital cost, operation, and maintenance cost, and electricity cost, respectively.  $E_{p,year}$  refers to the annual hydrogen production, which is calculated in the hypothetical scenario that the system constantly operates thorough the year. To levelized the costs on a yearly basis, the capital recovery factor (CRF) is introduced to account for time depreciation value. This parameter can be calculated as follows:

$$CRF = \frac{r \cdot (1 + r)^N}{[(1 + r)^N - 1]} \quad (11)$$

where  $r$  refers to the interest rate and  $N$  lifetime period. Accordingly, the annualized capital cost ( $\dot{Z}_{cc}$ ) mainly considers the electrolyzer cost ( $\dot{C}_{el}$ ) and storage cost ( $\dot{C}_{st}$ ):

$$\dot{Z}_{cc} = (\dot{C}_{el} + \dot{C}_{st}) \cdot CRF \quad (12)$$

Similarly, the annualized maintenance cost ( $\dot{Z}_{O\&M}$ ) can be calculated as follows [27]:

$$\dot{Z}_{O\&M} = (0.41 \cdot H^{-0.23}) \cdot CRF \quad (13)$$

where  $H$  represents the hydrogen production capacity (in kg H<sub>2</sub>/s). Finally, the annualized electricity cost ( $\dot{Z}_e$ ) can be calculated by relating the power consumption of the electrolyzer ( $P_{el}$ ) through the service time, as shown in eq. (14) [15]:

$$\dot{Z}_e = \eta_{AC/DC} \cdot \sum P_{el} \cdot \tau \quad (14)$$

where  $\eta_{AC/DC}$  refers to the AC/DC converter efficiency, and  $\tau$  is a constant that relates the electricity capacity factor at the given power condition. Table 7 list the main assumptions within the analysis.

Table 7.  
Results of the autodetonation for different operation modes.

Parameter	Value	Reference
Number of years, $N$	10 years	[26]
Converter efficiency, $\eta_{AC/DC}$	94%	[15]
Operating hours per year	7886 h	[14]
Escalating factor, $\alpha$	0.67	[22]
Annual interest rate [ $r$ ]	7%	[14]

Source: The authors.

## 4. Results and discussion

### 4.1 Electrolyzer

The first approximation of the experimental assessment is to evaluate the performance of the electrolyzer based on operational parameters. Fig. 6 shows the polarization curves obtained for the electrolyzer.

The results indicate that higher KOH concentration enhances the performance of the electrolyzer since less voltage is required to dissociate the water molecules. This pattern can be associated with the higher electrolytic conductivity that promotes reaction kinetics at the electrodes [26]. Overall, the cell voltage can be reduced between 4-15% by increasing the KOH concentration from 10 to 40 %p/p, which demonstrates the great dependence of the electrolyte concentration. Afterward, Fig. 7 shows the behavior of hydrogen production in the electrolyzer.

According to the results of Fig. 7, the hydrogen production features a direct relation to the operating current, whereas greater electrolyte concentrations boost the overall flow rate. However, the relative difference is limited to low-medium currents. Particularly, 40% and 30% electrolyte concentrations experience the highest production outcome.

On the other hand, Fig. 8 displays the electrolyzer efficiency for different KOH concentrations.

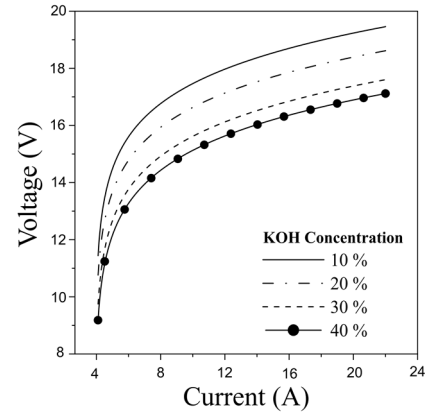


Figure 6. Polarization curve for the electrolyzer.  
Source: The authors.

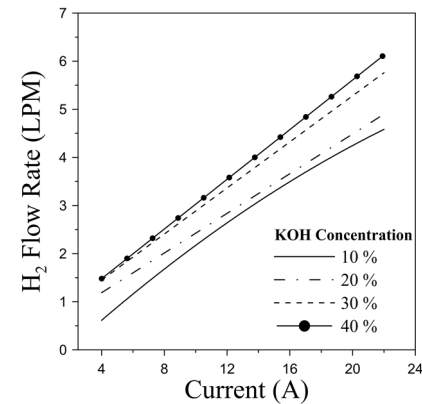


Figure 7. Effects of current and KOH concentration on hydrogen production.  
Source: The authors.

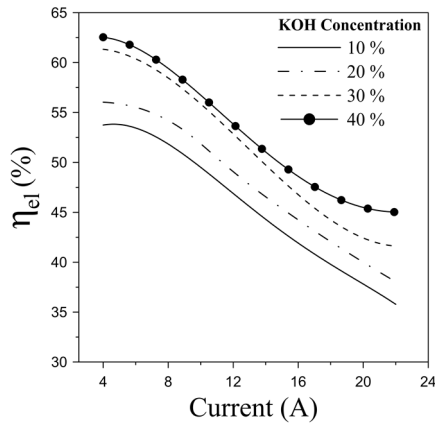


Figure 8. Electrolyzer efficiency.  
Source: The authors.

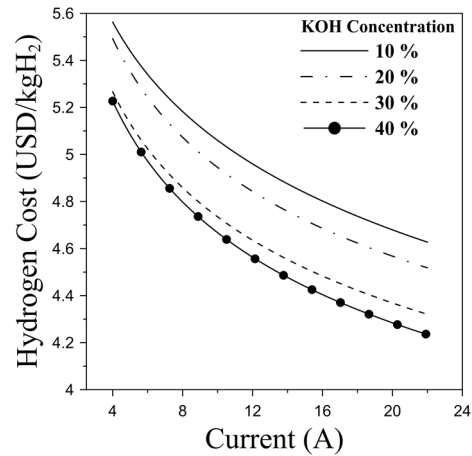


Figure 10. Electrolyzer efficiency.  
Source: The authors.

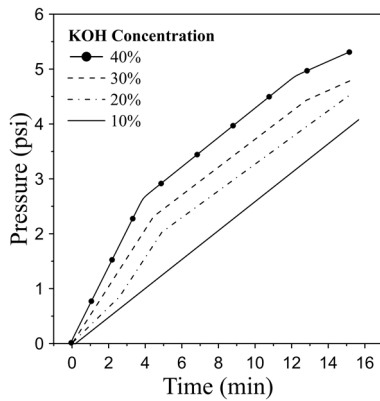


Figure 9. Effect of the KOH concentration on the hydrogen pressure.  
Source: The authors.

Fig. 8 indicates that the electrolyzer efficiency features a decreasing trend as the current rises. Also, higher KOH concentrations display a significant improvement in the electrolyzer's efficiency.

Particularly, the efficiency differential between the 40% and 30 % scenarios is not substantial at low-medium current rates. Overall, the efficiency varies between 55-40% for a wide operating range, which is consistent with the overall performance of this technology [15,26]. Higher hydrogen production demands (increasing current density) produce an increase in the cell voltage, which results in lower efficiency, as can be verified from Fig. 6 and 8. The sources of inefficiencies can be associated with the ionic resistivity in the electrolyte, electrode separation distance, and the presence of bubbles [14,22,25]. Subsequently, Fig. 9 illustrates the effect of the electrolyte concentration on the hydrogen pressure hydrogen within a time interval. Notice that the recorded time was established after 20 min to meet stability in the operation.

Based on the results, the hydrogen pressure experiences the best performance as the electrolyte concentration decreases. The pressure of the hydrogen produced increases over time until it reaches the maximum pressure of the storage tank (15 psi). These results are key to evaluate the performance of the electrolyzer, especially in the start-up

stage. The findings are consistent with the overall behavior reported by Kumar and Himabindu [6]. The parametric analysis performed from the experimental assessment demonstrates that the 30 %p/p KOH concentration features the best performance since both hydrogen production and electrolyzer efficiency remain at the highest levels. Even though the parameters mentioned above are slightly higher for a 40 %p/p at some operating range, the hydrogen pressure features the worst performance from the cases analyzed.

#### 4.1.1 Economic perspectives

The cost of hydrogen production for a specific electrolyzer technology is, by far, one of the most important economic metrics to evaluate the feasibility and viability of the proposal [7]. Hence, Fig. 10 shows the economic predictions for the present study using the KOH concentration as the comparison margin parameter.

The results indicate that cost of hydrogen production features a decreasing trend as the current increases. Additionally, higher electrolyte concentrations enable significant reductions in the overall cost. This pattern supported the results obtained from the last section. The overall cost varies from 4.23 USD to 5.58 USD, which is congruent with similar studies [2,7]. The results demonstrate that alkaline electrolyzers are competitive with other technologies such as PEM and solid oxide electrolyzers [1].

Notice that based on the application of the study, some cost intensifiers have been neglected, namely compression cost, gas conditioning, degradation, among others that are incorporated in the techno-economic analysis of hydrogen production plants. Despite some simplifications, this approach provides a wide perspective of the economic performance of alkaline electrolyzers for dual-fuel operation in internal combustion engines, which is rarely characterized in the literature. Since the economic approach is performed based on the operational parameters of the component, the impact of different system optimizations such as electrode material and separation distance can be easily evaluated on the production cost.



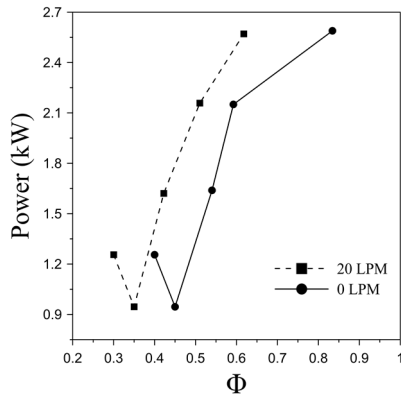


Figure 11. Effect of the equivalence ratio on the power output.  
Source: The authors.

#### 4.2 Combustion phenomena and fuel consumption

This section aims to discuss the essential aspects related to the combustion phenomena when operating in dual-fuel mode. Fig. 11 describes the power output behavior as a function of the equivalence ratio ( $\Phi$ ).

In general, it can be observed that the more demanding operation modes, in terms of power output, feature higher fuel consumption rates since the equivalence ratio reaches the rich zone as a result of the intake airflow is not throttled. Hence, whenever the equivalence ratio is reduced for the same operation mode, it produces a fuel consumption minimization.

To verify the influence of the operating margin and the dual-fuel operation, the fuel consumption metrics are analyzed. Fig. 12 displays the influence of the hydrogen energy share ( $\Omega$ ) on the BSDFC and the BFCE at different load rates.

Based on the outcomes, the BSDFC decreases as the presence of hydrogen rises, which demonstrates that hydrogen enrichment facilitates the energy demand for combustion, thus reducing fuel consumption. Also, it can be seen that higher load rates enable less hydrogen energy share, which is consistent with the results of the equivalence ratio.

Particularly, the highest BSDFC reduction was obtained by a load rate of 100%, whereas the 83% load rate features the lowest. Specifically, by increasing the hydrogen energy share from 0 to 16.13% at a load rate of 100%, the BSDFC dropped by approximately 220.06 g/kWh. This represents a minimization of fuel consumption of 30.85% when compared to the operation with the stand-alone biodiesel blend. The results are consistent with former research [8].

For the load rate of 83%, only a 4.04% reduction of the BSDFC can be obtained by increasing the  $\Omega$  from 0 to 30.94%. However, this loading rate features the lowest fuel consumption rate. In this sense, it can be verified that medium load conditions, namely 43 %, feature the highest consumption rate levels. In contrast, medium-high load rates (83%) experience the lowest BSDFC values, but the effect of hydrogen enrichment is not large. This demonstrates that the influence of hydrogen enrichment on the fuel consumption rate behavior is not quite intuitive as it is greatly affected by the operating conditions.

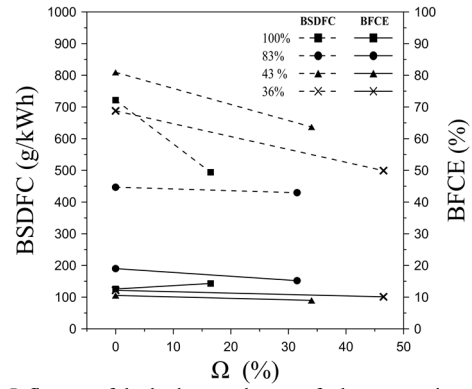


Figure 12. Influence of the hydrogen share on fuel consumption metrics  
Source: The authors.

On the other hand, the overall behavior of the BFCE presents a downward trend, excepting the 100% load rate. The reduction in fuel metrics can be related to the generated vapor as a consequence of hydrogen combustion and the autoignition delay of the biodiesel blend [14,5]. The latter appeared to be a significant factor since part of the energy produced during combustion is absorbed by this vapor, thus reducing the power of each cycle. Despite the negative effects of hydrogen enrichment, the average reduction does not overpass more than 4.4%. Also, considering that the dual-fuel operation contributes to reducing a great share of the greenhouse emissions and the BSDFC, a minimal sacrifice on the power output is reasonable [8].

#### 5. Conclusions

The present study introduced an experimental assessment of the overall performance of the dual-fuel operation, namely hydrogen injection and palm biodiesel blend (B10) in low displacement diesel engines. The proposed system integrated an in-house alkaline electrolyzer in the test bench for hydrogen enrichment. The study incorporated a complete characterization of the alkaline electrolyzer operation from a techno-economic perspective, which emerges as a novel contribution for partial fuel substitution applications.

The overall performance of the electrolyzer demonstrates that the electrolyte concentration (KOH) has a significant influence on operating variables such as current, voltage, and pressure. Specifically, higher electrolyte concentrations reduce the voltage required for electrolysis up to 15 %, which contributes to obtaining higher efficiencies and production rates. Specifically, a KOH concentration of 30 wt.% shows the best performance since both the hydrogen production and electrolyzer efficiency remain pretty close to the highest values (40 wt.%) while displaying intermediate hydrogen pressure values (3-4 psi). The exploration of the optimal operating temperature of the electrolyzer is recommended as a further step for improving the overall performance of this component.

The economic approach stands as a remarkable aspect that provides a framework for cost estimations in the dual-fuel operation of ICEs. The results showed that the hydrogen production price varies from 4.2 USD/kg to 5.2 USD/kg, which appears to be competitive with other green-hydrogen

technologies. The electrolyte has a significant impact on the overall cost since a higher concentration reduces the hydrogen cost between 2 – 8%. There is an open path for system optimization and cost minimization in electrode materials and separation distance.

According to the fuel consumption metrics, hydrogen enrichment of 20 LPM demonstrated promising results. Particularly, by incorporating hydrogen injection in the intake air, the BSDFC was reduced for all the operation modes since less fuel is necessary to meet the energy demand for combustion. Lower load rates enable higher values of hydrogen energy share. Accordingly, the maximum BSDFC reduction of nearly 31 % with hydrogen enrichment was obtained for a full load rate. However, the fuel consumption was not minimal. Indeed, even though the lowest BSDFC reduction (less than 5%) was obtained for a load rate of 83 %, it features the least fuel consumption rate with an average of 432.25 g/kWh. Meanwhile, a medium load rate (43%) experiences the highest fuel consumption rate with an average value of 723.44 g/kWh.

On the other hand, the second approach to the fuel consumption metrics revealed that hydrogen incorporation reduces the BFCE but in a minor proportion (<5%). This pattern can be associated with the vapor that is generated from hydrogen combustion, which absorbed part of the energy, thus reducing the power output. Another explanation could be found on the autoignition delay and injection times. An autoignition control mechanism is strongly recommended to reduce the undesired reduction in the fuel conversion efficiency.

In conclusion, the dual-fuel operation appeared to be a robust and reliable mechanism to reduce fuel consumption while maintaining appropriate thermo-mechanical performance. The simplicity and effectiveness of this technology are key features that promote its massive implementation. Alkaline electrolyzers have proven to be a practical and feasible component to provide zero-emissions hydrogen at reasonable costs.

## 6. Nomenclature

Symbol	Name	Unit
$m$	Mass	kg
$PM$	Molecular weight	kg/mol
$\Phi$	Equivalence ratio	-
$BSDFC$	Break specific dual fuel consumption	g/kWh
$BSFC$	Brake specific fuel consumption (diesel)	g/kWh
$BFCE$	Break specific fuel consumption efficiency	%
$\dot{m}$	Mass flow rate	kg/s
$P_{br}$	Break power	kW
$\Omega$	Hydrogen energy share	%
$LHV$	Low heating value	kWh/kg
$\dot{V}$	Volumetric flow	m <sup>3</sup> /s
$\rho$	Mass density	kg/m <sup>3</sup>
$V$	Voltage	V
$I$	Current	A
$Inv$	Investment cost	-
$CP$	Capacity factor	-
$\dot{C}$	Cost	USD
$\dot{Z}$	Annualized cost	USD/year
$E_{p,year}$	Annual production	kg/year
$CRF$	Capital recovery factor	-

$r$	Interest rate	%
$N$	Lifetime period	years
$H$	Hydrogen capacity	kg/year
$P_{el}$	Electrolyzer power consumption	kW
$\alpha$	Escalating factor	-
$\eta_{el}$	Electrolyzer efficiency	%
$\eta_{AC/DC}$	Converter efficiency	%
<b>Subscripts</b>		
$H_2$	Hydrogen	-
$act$	Actual	-
$cc$	Capital cost	-
$dual$	Dual-fuel operation	-
$el$	Electrolyzer	-
$e$	Electricity	-
$est$	Stoichiometric	-
$st$	Storage	-
$O\&M$	Operation and maintenance	-
$ref$	Reference	-

## References

- [1] Gutierrez, J.C., Valencia-Ochoa, G. and Duarte-Forero, J., Regenerative organic rankine cycle as bottoming cycle of an industrial gas engine: traditional and advanced exergetic analysis, *Applied Sciences*, 10(13), pp. 4411-4439, 2020. DOI: 10.3390/app1013441
- [2] Ochoa, G.V., Isaza-Roldan, C. and Duarte-Forero, J., Economic and Exergo-Advance analysis of a waste heat recovery system based on regenerative organic rankine cycle under organic fluids with low global warming potential, *Energies*, 13(6), pp. 1317-1338, 2020. DOI: 10.3390/en13061317
- [3] Bartan, A., Kucukali, S. and Ar, I., Environmental impact assessment of coal power plants in operation, *E3S Web of Conferences*, 22, pp. 00011-00019, 2017. DOI: 10.1051/e3sconf/20172200011
- [4] Krishna, S.M., Abdul-Salam, P., Tongroon, M. and Chollacoop, N., Performance and emission assessment of optimally blended biodiesel-diesel-ethanol in diesel engine generator, *Applied Thermal Engineering*, 155, pp. 525-533, 2019. DOI: 10.1016/j.applthermaleng.2019.04.012
- [5] Maestre-Cambronel, D., Guzmán-Barros, J., Gonzalez-Quiroga, A., Bula, A. and Duarte-Forero, J., Thermoeconomic analysis of improved exhaust waste heat recovery system for natural gas engine based on Vortex Tube heat booster and supercritical CO<sub>2</sub> Brayton cycle, *Sustainable Energy Technologies and Assessments*, 47, pp. 101355-101371, 2021. DOI: 10.1016/j.seta.2021.101355
- [6] Zhang, W., Maleki, A., Rosen, M.A. and Liu, J., Sizing a stand-alone solar-wind-hydrogen energy system using weather forecasting and a hybrid search optimization algorithm, *Energy Conversion and Management*, 180, pp. 609-621, 2019. DOI: 10.1016/j.enconman.2018.08.102
- [7] Ferrero, D., Gamba, M., Lanzini, A. and Santarelli, M., Power-to-Gas hydrogen: techno-economic assessment of processes towards a multi-purpose energy carrier, *Energy Procedia*, 101, pp. 50-57, 2016. DOI: 10.1016/j.egypro.2016.11.007
- [8] Milani, D., Kiani, A. and McNaughton, R., Renewable-powered hydrogen economy from Australia's perspective, *International Journal of Hydrogen Energy*, 45(21), pp. 24125-24145, 2020. DOI: 10.1016/j.ijhydene.2020.06.041
- [9] Sathiyamoorthi, R., Sankaranarayanan, G., Adhith-Kumaar, S.B., Chiranjeevi, T. and Dilip-Kumar, D., Experimental investigation on performance, combustion and emission characteristics of a single cylinder diesel engine fuelled by biodiesel derived from Cymbopogon Martini, *Renewable Energy*, 132, pp. 394-415, 2019. DOI: 10.1016/j.renene.2018.08.001
- [10] Mejía, A., Leiva, M., Rincón-Montenegro, A., Gonzalez-Quiroga, A. and Duarte-Forero, J., Experimental assessment of emissions maps of a single-cylinder compression ignition engine powered by diesel and palm oil biodiesel-diesel fuel blends, *Case Studies in Thermal Engineering*, 19, pp. 100613-100625, 2020. DOI: 10.1016/j.csite.2020.100613
- [11] Guillin-Estrada, W., Maestre-Cambronel, D., Bula-Silvera, A., Gonzalez-Quiroga, A. and Duarte-Forero, J., Combustion and

- performance evaluation of a spark ignition engine operating with Acetone-Butanol-Ethanol and Hydroxy, *Applied Sciences*, 11(11), pp. 5282-5309, 2021. DOI: 10.3390/app11115282
- [12] Ferreira, B.E.P., Moreira, V.G., Nazareno, T.G. and Hanriot, S. de M., The effects of injection pressure and energizing time on the combustion of an engine fueled with diesel oil and ethanol blend. In: 2020 SAE Brasil Congress & Exhibition, 2021.
- [13] Uyumaz, A., Aydoğan, B., Solmaz, H., Yılmaz, E., Yeşim Hopa, D., Aksoy Bahtli, T., Solmaz, Ö. and Aksoy, F., Production of waste tyre oil and experimental investigation on combustion, engine performance and exhaust emissions, *Journal of the Energy Institute*, 92(5), pp. 1406-1418, 2019. DOI: 10.1016/j.joei.2018.09.001
- [14] Kuckshinrichs, W., Ketelaer, T. and Koj, J.C., Economic analysis of improved alkaline water electrolysis, *Frontiers in Energy Research*, 5, 2017. DOI: 10.3389/fenrg.2017.00001
- [15] Nistor, S., Dave, S., Fan, Z. and Sooriyabandara, M., Technical and economic analysis of hydrogen refueling, *Applied Energy*, 167, pp. 211-220, 2016. DOI: 10.1016/j.apenergy.2015.10.094
- [16] Aparicio, G.M., Vargas, R.A. and Bueno, P.R., Protonic conductivity and thermal properties of cross-linked PVA/TiO<sub>2</sub> nanocomposite polymer membranes, *Journal of Non-Crystalline Solids*, 522, pp. 119520-119527, 2019. DOI: 10.1016/j.jnoncrysol.2019.119520
- [17] Escobar-Yonoff, R., Maestre-Cambronel, D., Charry, S., Rincón-Montenegro, A. and Portnoy, I., Performance assessment and economic perspectives of integrated PEM fuel cell and PEM electrolyzer for electric power generation, *Heliyon*, 7(3), art. e06506, 2021. DOI: 10.1016/j.heliyon.2021.e06506
- [18] Mehra, R.K., Duan, H., Luo, S., Rao, A. and Ma, F., Experimental and artificial neural network (ANN) study of hydrogen enriched compressed natural gas (HCNG) engine under various ignition timings and excess air ratios, *Applied Energy*, 228, pp. 736-754, 2018. DOI: 10.1016/j.apenergy.2018.06.085
- [19] Siddiqui, O. and Dincer, I., Design and assessment of a new solar-based biomass gasification system for hydrogen, cooling, power and fresh water production utilizing rice husk biomass. *Energy Conversion and Management*, 236, pp. 114001-114013, 2021. DOI: 10.1016/j.enconman.2021.114001
- [20] Ulleberg, O., Modeling of advanced alkaline electrolyzers: a system simulation approach, *International Journal of Hydrogen Energy*, 28(1), pp. 21-33, 2003. DOI: 10.1016/S0360-3199(02)00033-2
- [21] Thiagarajan, S., Sonthalia, A., Edwin Geo, V. and Chokkalingam, B., Effect of waste exhaust heat on hydrogen production and its utilization in CI engine, *International Journal of Hydrogen Energy*, 45(10), pp. 5987-5996, 2020. DOI: 10.1016/j.ijhydene.2019.06.032
- [22] Yao, J., Kraussler, M., Benedikt, F. and Hofbauer, H., Techno-economic assessment of hydrogen production based on dual fluidized bed biomass steam gasification, biogas steam reforming, and alkaline water electrolysis processes, *Energy Conversion and Management*, 145, pp. 278-292, 2017. DOI: 10.1016/j.enconman.2017.04.084
- [23] Gupta, H.: *Fundamentals of internal combustion engines*. 2012
- [24] Amador, G., Forero, J.D., Rincon, A., Fontalvo, A., Bula, A., Padilla, R.V. and Orozco, W., Characteristics of Auto-Ignition in internal combustion engines operated with gaseous fuels of variable methane number, *Journal of Energy Resources Technology*, 139(4), pp. 042205-042212, 2017. DOI: 10.1115/1.4036044
- [25] Karagöz, Y., Balci, Ö., Orak, E. and Habib, M.S., Effect of hydrogen addition using on-board alkaline electrolyser on SI engine emissions and combustion, *International Journal of Hydrogen Energy*, 43, pp. 11275-11285, 2018. DOI: 10.1016/j.ijhydene.2018.04.235
- [26] David, M., Ocampo-Martínez, C. and Sánchez-Peña, R., Advances in alkaline water electrolyzers: a review, 2019.
- [27] Yilmaz, C., Kanoglu, M., Bolatturk, A. and Gadalla, M., Economics of hydrogen production and liquefaction by geothermal energy, *International Journal of Hydrogen Energy*, 37(2), pp. 2058-2069, 2012. DOI: 10.1016/j.ijhydene.2011.06.037
- [28] Saravanan, P., Kumar, N.M., Ettappan, M., Dhanagopal, R. and Vishnupriyan, J., Effect of exhaust gas re-circulation on performance, emission and combustion characteristics of ethanol-fueled diesel engine, *Case Studies in Thermal Engineering*, 20, pp. 100643-100652, 2020. DOI: 10.1016/j.csite.2020.100643

**D. Maestre-Cambronel**, received his BSc. Eng. in Mechanical Engineering in 2020 and Spc. in Efficient Energy Management in 2021, from the Universidad del Atlántico, Barranquilla-Colombia. Currently, he is a researcher of the KAI Research Unit from the Universidad del Atlántico. His research interests include: thermal systems; Hydrogen technologies; ICEs; Power generation; Techno-economic optimization of energy systems. ORCID: 0000-0002-0390-1555

**B. Hernández-Comas**, received the BSc. Eng. in Mechanical Engineering in 2020 from the Universidad del Atlántico, Barranquilla-Colombia. Currently, he is a researcher of the KAI Research Unit from the Universidad del Atlántico. His research interests include: energy systems; ICEs; Thermoelectric generators; computational fluid dynamics. ORCID: 0000-0002-9702-4150

**J. Duarte-Forero**, Barranquilla native, Colombia. He is an associated professor of the Mechanical Engineering Program at Universidad del Atlántico, Barranquilla, Colombia. He received his BSME from Universidad del Atlántico, Barranquilla, Colombia in 2007. MSc. in Mechanical Engineering from Universidad del Norte, Barranquilla, Colombia in 2013. PhD. in Engineering from Universidad del Norte, Colombia in 2017. He is a COLCIENCIAS - Senior Researcher. ORCID: 0000-0001-7345-9590